HHS Public Access

Author manuscript

J Neurochem. Author manuscript; available in PMC 2019 September 01.

Published in final edited form as:

J Neurochem. 2018 September ; 146(6): 753–766. doi:10.1111/jnc.14539.

HCN channels in the hippocampus regulate active coping behavior

Mr. Daniel W. Fisher[#1], **Ye Han**[#1], **Kyle A. Lyman**[#1], **Robert J. Heuermann**[1,2], **Linda A. Bean**[3], **Natividad Ybarra**[3], **Kendall M. Foote**[1], **Hongxin Dong**[4], **Daniel A Nicholson**[3], and **Dane M. Chetkovich**[1,5]

[1]Davee Department of Neurology and Clinical Neurosciences, Northwestern University Feinberg School of Medicine, Chicago, IL 60611 USA

[2]Department of Neurology, Washington University School of Medicine, St. Louis, MO, 63110 USA

[3]Department of Neurological Sciences, Rush University Medical Center, Chicago, IL, 60611 USA

[4]Department of Psychiatry & Behavioral Sciences, Northwestern University, Feinberg School of medicine, Chicago, IL 60611, USA

[5]Department of Neurology, Vanderbilt University Medical Center, 1161 21st Ave South, A1124-A MCN, Nashville, TN 37232 USA

[#] These authors contributed equally to this work.

Abstract

Active coping is an adaptive stress response that improves outcomes in medical and neuropsychiatric diseases. To date, most research into coping style has focused on neurotransmitter activity and little is known about the intrinsic excitability of neurons in the associated brain regions that facilitate coping. Previous studies have shown that HCN channels regulate neuronal excitability in pyramidal cells and that HCN channel current (I_h) in the CA1 increases with chronic mild stress. Reduction of I_h in the CA1 leads to antidepressant-like behavior, and this region has been implicated in the regulation of coping style. We hypothesized that the antidepressant-like behavior achieved with CA1 knockdown of I_h is accompanied by increases in active coping. In this report, we found that global loss of TRIP8b, a necessary subunit for proper HCN channel localization in pyramidal cells, led to active coping behavior in numerous assays specific to coping style. We next employed a viral strategy using a dominant negative TRIP8b isoform to alter coping behavior by reducing HCN channel expression. This approach led to a robust reduction in I_h in CA1 pyramidal neurons and an increase in active coping. Together, these results establish that changes in HCN channel function in CA1 influences coping style.

Abstract

Contact Information: 1161 21st Ave South, A1124-A MCN, Nashville, TN 37232 USA. dane.m.chetkovich@vanderbilt.edu.

Conflict of Interest

The authors declare no conflicts of interest.

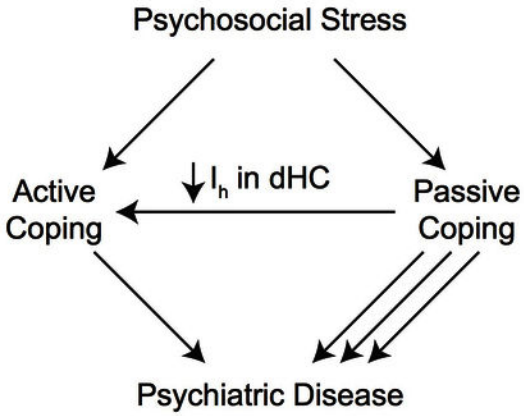

Active coping is an adaptive stress response that improves outcomes in medical and neuropsychiatric diseases. To date, most research into coping style has focused on neurotransmitter activity and little is known about the intrinsic excitability of neurons in the associated brain regions that facilitate coping. Previous studies have shown that HCN channels regulate neuronal excitability in pyramidal cells and that HCN channel current (Ih) in the dorsal hippocampal (dHC) CA1 increases with chronic mild stress. In this report, we found that global loss of TRIP8b, a necessary subunit for proper HCN channel localization in pyramidal cells, led to active coping behavior in numerous assays specific to coping style. Using a viral strategy in CA1 to knockdown Ih via a dominant negative TRIP8b isoform, we achieved an increase in active coping through greatly reduced Ih in these CA1 pyramidal cells. Together, these results establish that changes in HCN channel function in CA1 influences coping style.

Introduction

By 2030, Major Depressive Disorder (MDD) will be 1 of 3 leading causes of disease burden worldwide, with a lifetime incidence of 10–15%(Mathers & Loncar 2006, Briley & Lépine 2011, Weissman Mm 1996, Kessler Rc 2005) and a tremendous economic impact [reviewed in Briley and Lapine 2011]. There is increasing interest in abnormal connectivity within cortico-limbic circuitry in MDD as well as the morphological, molecular, and electrophysiological changes underlying these circuit dysfunctions(Arnone *et al.* 2012, Duman & Aghajanian 2012, Duman & Monteggia 2006, Krishnan & Nestler 2008). Of these changes, molecular regulators of neuronal excitability are likely to influence MDD.

One important regulator of neuronal activity is the hyperpolarization-activated cyclic nucleotide-gated (HCN) channel(Hu *et al.* 2002, Narayanan & Johnston 2007, Narayanan & Johnston 2008, Fan *et al.* 2005, Brager & Johnston 2007). HCN channels mediate a nonspecific cationic current (I_h) that is active at the resting membrane potential in CA1 pyramidal neurons. Because of its effect on membrane resistance, I_h is critical for controlling neuronal excitability and regulating synaptic inputs(Narayanan & Johnston 2007, Marcelin *et al.* 2012, Nolan *et al.* 2007, Nolan *et al.* 2004, Nolan *et al.* 2003, Schaefer *et al.* 2006). Further, HCN channels are expressed at significantly higher levels in the distal

dendrites of CA1 pyramidal neurons where they play a crucial role in regulating temporal summation(Magee 1998, Lewis *et al.* 2011). This distribution of HCN channels is regulated by an auxiliary subunit, tetratricopeptide repeat-containing Rab8b-interacting protein (TRIP8b), and loss of this localizing protein ablates HCN channel distal dendritic enrichment and reduces HCN channel surface expression(Lörincz *et al.* 2002, Lewis et al. 2011).

Recently, our lab and others have shown that knock-out (KO) of the major pore-forming HCN channel subunits (HCN1 or HCN2) or TRIP8b leads to an antidepressant-like phenotype in mice on the Forced Swim Test (FST) and Tail Suspension Test (TST)(Kim *et al.* 2012, Han *et al.* 2017, Lewis et al. 2011). Kim and colleagues(Kim *et al.* 2017) showed that HCN1 in the CA1 is increased with chronic mild stress and that shRNA knockdown of HCN1 in the CA1 leads to a reduction in anhedonia-like behavior and an increase in antidepressant-like behavior. Importantly, our lab has demonstrated that specific loss of distal dendritic HCN improves performance on both the FST and TST and that rescue of this enrichment specifically in the CA1 is sufficient to reverse this antidepressant-like phenotype(Han et al. 2017).

Though previous studies have emphasized individual differences in susceptibility and resilience to developing pathological behaviors under chronic stress (i.e. depression-like behaviors)(Russo *et al.* 2012), fewer studies have examined how individual animals adapt and respond to acute stressors. An individual's tendency towards certain responses to acute stress is often described as coping style, and two overarching categories are often described in both the human and rodent literature: active and passive coping(Southwick *et al.* 2005, Koolhaas *et al.* 2010). In rodents, active coping behaviors are thought to be reflected in the ability of the rodent to reduce the impact of acute stressors through directly addressing them. One example of this is a rodent's tendency to reduce the stressfulness of an electrified probe by actively burying as opposed to passively avoiding it(De Boer & Koolhaas 2003, Koolhaas et al. 2010). Importantly, patients with strong active coping tendencies show resistance to psychiatric illness and more favorable outcomes during treatment of chronic illnesses of all types, and studies have shown that active coping behaviors in rodents are correlated with decreased depression-like behaviors after chronic stress(Wood *et al.* 2010, Vidal *et al.* 2011).

We hypothesized that loss of I_h in the CA1 could lead to antidepressant-like changes as a component of a broader active coping phenotype. To test this, we subjected *Trip8b*$^{+/+}$ and *Trip8b*$^{-/-}$ mice to a number of coping assays, including the Two-Way Active Avoidance Test (2w-AA), the Resident-Intruder Test (RIT), Shock Probe Burying Test (SPBT), and the Repeated Forced Swim Test (rFST). To target HCN channels in CA1 more specifically, we used a viral approach to reduce I_h in wild type mice through expression of a dominant negative TRIP8b isoform in CA1.

Materials and Methods (Detailed methods in Supplementary Materials)

Animals

Global *Trip8b*$^{-/-}$ mice creation and genotyping have been previously described(Lewis et al. 2011). Although we have previously referred to these animals by the name of the gene

encoding TRIP8b protein (*Pex5l*), we have elected to refer to the gene as *Trip8b* in this manuscript for clarity. Male 8 to 16 week-old *Trip8b*$^{+/+}$ and *Trip8b*$^{-/-}$ mice were used for all studies, as many of the coping assays, especially those measuring aggression, are not appropriate for female mice. For electrophysiology and virus experiments, wildtype C57Bl/6J (RRID:IMSR_JAX:000664) mice were obtained from Jackson Laboratories (Bar Harbor, Mn) at 8 weeks-old. Mice were maintained on a 12:12 hour light:dark cycle, with food and water given *ad libitum*. Mice weighed 20–30g at time of assaying. All animal experiments were performed according to protocols approved by the Institutional Animal Care and Use Committees of Northwestern University (protocol IS00000356) and was not pre-registered.

Virus

The DNA plasmid for *pAAV-hsynapsin-Cre-IRES-eGFP* was kindly provided by Dr. Pavel Osten (Cold Spring Harbor Laboratory), as in our previous report(Han et al. 2017). The TRIP8b(1b-2) isoform was then subcloned into this vector, and AAV serotype 2/8 vectors were produced by the Gene Therapy Program of the University of Pennsylvania.

Stereotaxic Viral Injection

Injection of viral vectors were done as previously described(Han et al. 2017). Briefly, mice were anesthetized with inhalational isoflurane and mounted on a stereotaxic instrument (Stoelting, Wood Dale, IL). A midline incision was made at the scalp, and a small craniotomy was performed with a dental drill. 1μl of 3×10^{12} vector genome (vg)/ml of AAV was injected into the dorsal CA1 (2.3 mm A/P, ±1.3 mm M/L, −1.7 D/V) of C57BL/6J mice at a rate of 0.3 μl/min via a 5 μl Hamilton syringe. After the injection, the needle was left in place for 5 minutes to allow the virus to diffuse before removing the needle at a rate of 1 mm/min. A minimum of 4 weeks was allowed to pass between injection and experimentation in order for maximal viral expression. For a detailed description of the extent of viral spread, please see our previous report where identical conditions and techniques were used(Han et al. 2017).

Behavioral Testing

Before each behavioral task, the mice were acclimated to the behavioral testing room for at least 1 hr. All tests were performed in an isolated room under quiet conditions, and all behavioral experiments took place during the light phase of the light:dark cycle. For experiments with multiple trials over many days, each trial occurred within 2 hours of the same time each day. For serial behavioral tasks, at least 4 days were allowed for the mice to recover before the next test. All behavioral testing apparatuses were cleaned with 70% ethanol between trials. All experimenters were blind to the subjects' groups during testing and analysis; a technician who was not otherwise involved in the experiments randomized (simple randomization) subjects before testing. Behavioral tests using these parameters are described below and include the Open Field Test, Zero Maze, Morris Water Maze, Two-Way Active Avoidance, Resident Intruder Test, Shock Probe Burying Test, and repeated Forced Swim Test.

Open Field Test (OFT)

The OFT was performed as previously described(Han et al. 2017). Briefly, each mouse was placed in a 60cm plastic arena with white light illuminating the center of the arena. Mice were allowed to explore the arena for 10 minutes, and the time spent in the center and periphery of the arena as well as total distance traveled were recorded with overhead cameras and analyzed with Limelight 4.0 software (Coulbourne).

Zero Maze (ZM)

Each mouse was placed in a circular apparatus with 4 quadrants containing 2 closed and 2 open arms that alternated. The mouse was placed in the closed arms, the time spent in each arm was recorded for 5 minutes with an overhead camera, and behavior was analyzed with Limelight 4.0 software. If a mouse leapt from the zero maze, the mouse was not included in the later analysis.

Morris Water Maze (MWM)

The MWM was done similarly to our previous publication(Lewis et al. 2011), with minor deviations. The MWM consisted of tests in three phases: 4 days of visible platform training, 5 days of hidden platform training, and a probe trial which occurred before the hidden platform trials on the last 3 days of hidden platform testing (3 trials total over 3 days). The MWM consisted of a 120cm diameter circular pool filled with 24°C ± 1°C water that was made opaque with white, non-toxic paint. Around the arena, different shaped cues corresponding to the 4 cardinal directions were prominently displayed during the hidden platform and probe trials. Each day of training consisted of 4 trials per mouse per day with >60s inter-trial intervals. Probe trials were single trials when performed. Mice were placed in one of four starting locations facing the pool wall and allowed to swim freely until finding a 10 × 10 cm platform submerged in water by ~1 cm (hidden and probe) with a cutoff of 60 s. During the visible platform trials, the platform had four 1 cc syringes on the corner of the platform and was just at water level. If the mouse failed to find the platform within 60 s, the experimenter guided the mouse to the platform location. For each trial, the mouse was allowed to remain on the platform for 20s before the experimenter returned the mouse to its homecage. All behavior was tracked with overhead cameras and analysis was done using Actimetrics Water Maze. Average latency to reach the platform and distance traveled to the platform were the final endpoints for the hidden trials while average time spent in each quadrant represented the final endpoint for the probe trial.

Two-Way Active Avoidance (2w-AA)

The mice were tested in a two-way shuttle-box (Habitest; Coulbourne) equipped with an electrified grid floor and infrared sensors in each chamber. The 2w-AA consisted of 5 trials, each occurring daily, with each trial containing 30 active avoidance challenges per subject. The set-up for each trial was as follows: The arena was dimly lit, and the mouse was placed on the same side of the arena each day with the guillotine door open, allowing for free exploration. Each mouse was given 3 minutes to acclimate and explore the arena before the guillotine door closed, and the first challenge began. Each challenge began with the guillotine door raising and presentation of a 4kHz tone (65dB) and a 15W cue light on both

sides of the arena. If the moues transitioned to the adjacent chamber within 8s, the challenge was counted as an “Avoidance,” and the tone and cue light turned off, followed by an inter-trial interval (ITI) of 20–40s with the guillotine door closed. If the mouse failed to move within 8s of the cue onset, a 0.3mA scrambled shock was delivered for 5s. If the mouse transitioned to the adjacent chamber within this time, the trial was counted as an “Escape,” and the tone and cue turned off, followed by the ITI. If the mouse fails to move within 5s, the cue and shock were both stopped, and the trial was counted as a “Failure.” An ITI began before the next trial. The average counts of “Avoidance” were the main endpoints for this assay, as “Failures” were exceedingly rare.

Active Coping Index (ACI)

Three behavioral tasks to specifically assess active coping(Koolhaas et al. 2010) were administered to a single cohort of mice. These three tests are rarely or never used to describe depression-like behavior, specifically. The tests went in increasing order of stressfulness, starting with the Resident Intruder Test (RIT), Shock Probe Burying Test (SPBT), and Repeated Forced Swim Test (rFST). 2 weeks before testing, each mouse was housed individually and allowed to acclimate to their surroundings. At 1 week before testing, a wildtype female mouse was added to reduce the effects of isolation stress. This housing paradigm ensured sufficient territoriality of the subjects for the RIT and was maintained throughout the three assays.

Resident Intruder Test

The RIT was performed similar to previous publications(Koolhaas *et al.* 2013). Briefly, at 15 min prior to testing, the female was removed, and a clear plexiglass cage top replaced the normal food hopper to allow for clear visualization of the mice by a video recorder placed overhead. A 10 min trial began when a 6–8wk old male intruder was placed in the cage, and the resultant behavior was recorded. After the trial, the intruder was removed, food hopper replaced, and female put back in the cage. Videos were documented for numerous behaviors: Aggressive Behaviors (Lateral Threat, Upright, Clinch/Bite, Keep Down, Chase), Social Behaviors (Social Exploration, Ano-Genital Sniff, Social Grooming, Mounting), Exploratory Behaviors (Sniffing, Rearing, Cage Exploration), Defensive/Submissive Behaviors (Being Groomed, Fleeing, On Back, Submissive Freeze, Defensive Sideways, Defensive Upright) and other (Inactivity/Resting, Grooming, Digging). Aggressive behavior and attack latency were the main endpoints of this assay (averaged over daily trials for 3 days).

Shock Probe Burying Task

The SPBT was performed similar to previous publications(Degroot & Nomikos 2004). Briefly, all trials took place in a 13 × 11 × 17cm plexiglass arena with about 3cm of standard cage bedding (clean wood shavings). The arena was placed in an isolation cubicle (Coulbourne), and behavior was monitored by overhead video camera remotely. A 3 trial test was administered to each mouse over 3 days. During the first day, the mouse underwent an Acclimation Trial of 15 min, where they were placed in the arena without a shock probe and could explore freely. The second day, an Acquisition Trial was administered, where the subject was placed in the arena with a shock probe (4cm × 1cm cylinder; 0.5mA). The probe

was controlled manually by the experimenter and remained off unless the experimenter pushed a trigger. The probe was only electrified when the mouse made clear contact with the probe. The mouse explored the arena until it touched the probe with both paws and then was given its first shock. The resultant behavior was documented for the next 15 min of the trial, and the mouse was then returned to its homecage. There was no difference in the number of shocks received between groups (data not shown). On the third day, a Recall Trial was administered, where the subject was placed in the SPBT chamber with the shock probe, but it was never electrified. The mouse's behavior was documented for 15 min from the moment it entered the arena. Behaviors observed included burying, immobility (no ambulation with only occasional side to side, scanning movements of the head), ambulation, prod exploration (snout pointed towards the probe and sniffing), grooming, and rearing. The times spent burying and immobile as well as the latency to bury were the major endpoints for this assay during the Acquisition and Recall Trials. A "Change in Response" value was computed to determine if the mice showed differences in memory between the Acquisition and Recall Trial. The Change in Response was calculated by subtracting the total time spent freezing and burying in the Recall Trial from the total amount of time freezing and burying in the Acquisition Trial and dividing by the total time spent freezing and burying in the Acquisition Trial to get a ratio of the difference between trials normalized to the original amount of freezing and burying in the original trial.

Repeated Forced Swim Test

The rFST was performed similar to previous publications(Boucher *et al.* 2011). Briefly, each trial consisted of a 6 min immersion in a 4L beaker of tap water at a temperature of 24 +/− 1°C, and a daily trial was administered for three days. An observer recorded the amount of time the mouse remained immobile (no purposeful movements other than those necessary to remain afloat) during each trial during two time periods: the first two minutes and the last four minutes. For the "classical" FST measurements, the last four minutes of the first trial were scored for total time spent immobile. For the rFST, the full 6 minutes of each trial were scored over all three trials, and the average time spent immobile across trials was the main endpoint of this assay.

Z-score normalization

A large source of irreproducibility within behavioral neuroscience likely comes from the use of a Single Point In Time assay (SPIT). In addition to needing more subjects to uncover significant findings, SPIT is more susceptible to being influenced by unforeseen environmental factors and random chance. The z-score normalization method is used to reduce variability among many similar behavioral assays to get a more accurate account of a single behavioral domain. Similar to the Research Domain Criteria (RDoC) introduced by the NIMH, this method aims to better describe how individual performances on multiple, similar behavioral tasks that constitute overall behavior in a single domain – in this case, active coping(Casey *et al.* 2013, Insel *et al.* 2010). In addition, assays with multiple endpoints that measure different aspects of a particular behavior can be averaged together to give a z-score for the assay, such as was done for attack latency and time spent in offensive aggression for the RIT. In order to achieve an "index" for active coping, each individual assay's endpoints were converted into a z-score based on the normal distribution of the

wildtype population. In essence, this converts all the data within an assay into a single value with a single “unit” of measurement based on the relative performance of each individual to the average performance of the control group. This not only greatly reduces individual test variability but also reveals a more rigorously defined assessment of how an individual mouse tends to behave. The following formula was used to compute z-scores:

$$Z = (x_{subject} - \mu_{control})/\sigma_{control}$$

Where $x_{subject}$ = individual endpoint value, $\mu_{control}$ = control population average and $\sigma_{control}$ = standard deviation. Control refers to either the *Trip8b*$^{+/+}$ or AAV-GFP populations.

To prevent weighting one assay more than another, multiple endpoints within the same assay were first z-score normalized and then averaged together, yielding a single composite z-score per assay. To make sure all z-scores were consistent, each endpoint’s z-score was normalized so that a score > 0 depicted a tendency towards more active coping and a score < 0 depicted a tendency towards more passive coping. For instance, as a low latency for aggression is indicative of increased active coping, and the untransformed z-score for aggression demonstrates that negative scores had the lowest latencies (i.e. most aggression), the sign was flipped for this endpoint before the average for the assay was taken. A description of the combined endpoints within each assay to create the assay-specific indices are as follows: The Aggression Index consisted of average attack latency and average % time of offensive aggression. The SPBT Index consisted of the % time burying, % time freezing, and the latency to bury from both the Acquisition and Recall Trials (6 endpoints in total). The rFST index was solely comprised of the average immobility times across the three trials. The final ACI was then derived from the average of the assay indices.

Electron Microscopy

The distribution of HCN1 channel protein was examined using serial section, pre-embedding, silver-intensified, ultra-small immunogold electron microscopy as described previously (PESIUSIGEM; Lörincz et al., 2002; Dougherty et al., 2013). Briefly, mice receiving AAV-GFP injections or injections of AAV-(1b-2) were perfused with room temperature 0.9% saline, followed by acidic sodium acetate-buffered 2% paraformaldehyde/1% glutaraldehyde (pH = 6.0), then basic sodium borate-buffered 2% paraformaldehyde/1% glutaraldehyde (pH = 9.0). Slices were taken of the dorsal hippocampus, rinsed in Tris-buffered saline (TBS), exposed to 1% NaBH4, rinsed in TBS, blocked, and then incubated in lab-generated anti-HCN1 antibody (Shin et al., 2008). After rinsing in TBS, slices were blocked again and incubated in ultra-small immunogold particles (Aurion, Electron Microscopy Sciences), followed by rinsing in TBS, fixation of immunogold particles in 2% glutaraldehyde in phosphate-buffered saline (PBS), silver enhancement using the R-Gent SE-EM Enhancement Kit (Aurion), then osmication, and curing in Araldite 502. Polymerized slivers of CA1 were then dissected from slices, re-embedded, and rotated orthogonally to the plane of sectioning. Arrays of serial ultrathin sections (65 nm, as estimated using Small’s Method of Minimal Folds) were then collected using a Leica UC6 ultramicrotome and a diamond knife, followed by counterstaining in 5%

aqueous uranyl acetate and Reynold's lead citrate. Images were obtained at 7,500× or 10,000× magnification using a JEOL 1200EX transmission electron microscope or a Sigma HD VP scanning electron microscope in scanning-transmission (STEM) mode (Zeiss), respectively.

Statistics

All statistical calculations were performed using GraphPad 6 and MATLAB. All behavioral data that followed a normal distribution had outliers removed if they were > 2 standard deviations away from the population mean to avoid Type II errors(Peña *et al.* 2017). For pairwise comparisons, a two-tailed student's T-test was performed. For comparisons with two factors, a Two-Way ANOVA was used, and a Repeated Measures ANOVA was implemented when one of the factors was within subject (i.e. trials). Sidhak's *post-hoc* test was used as needed for pairwise comparisons following significant ANOVA results. Sample sizes were estimated based on results from previous publications or through power analysis based on preliminary cohort data with a power of 80% to achieve a 1SD difference at alpha = 0.05. The number of biological replicates per group are expressed as n-values in the captions for each figure. Significance was denoted with an asterisk, representing a p-value < 0.05, and all values were reported as mean±S.E.M.

Please see supplementary material for additional methods.

Results

Trip8b$^{-/-}$ mice show increased active coping in the Two-Way Active Avoidance Test (2w-AA)

Loss of HCN channel distal dendritic enrichment through elimination or suppression of endogenous TRIP8b expression has been shown to increase antidepressant-like behavior in rodents(Han et al. 2017, Lewis et al. 2011). To determine whether loss of this distal dendritic enrichment affects active coping, we subjected *Trip8b*$^{-/-}$ mice and *Trip8b*$^{+/+}$ to 2w-AA, a well-validated test of active coping. In this test, mice are placed in a two-chambered shock arena with a door allowing shuttling between the two chambers. During an AA trial, the door lifts and a light and tone cue are presented, encouraging the mouse to shuttle to the other chamber. If the mouse fails to move, a low-intensity shock is delivered. Mice that are naturally more active copers will show more avoidances to the cue than passive copers, which refrain from moving until the shock is administered(Koolhaas et al. 2010). Consistent with our hypothesis, we found that *Trip8b*$^{-/-}$ mice showed more avoidances on the first day of testing than their *Trip8b*$^{+/+}$ counterparts (Figure 1A,B). In addition, we observed that both *Trip8b*$^{-/-}$ and *Trip8b*$^{+/+}$ mice were able to learn to increase their avoidances over the following days of the trial, ultimately leading to >90% successful avoidance rate in both groups. This suggests that while *Trip8b*$^{-/-}$ mice show an inherently increased propensity for active coping, both groups are able to successfully learn to cope actively.

Trip8b$^{-/-}$ mice show increased active coping on a behavioral battery that specifically tests coping style

2w-AA directly assays active coping, but it remains unknown if *Trip8b*$^{-/-}$ mice show other signs of increased active coping in assays with more complex possible responses. For instance, while the 2w-AA favors active coping and punishes passive coping, the Shock Probe Burying Test (SPBT) measures active and passive coping behaviors without reinforcement of one or the other(De Boer & Koolhaas 2003). Further, improved performance on the 2w-AA may demonstrate that *Trip8b*$^{-/-}$ mice learn to actively cope more quickly within the first trial, which could reflect a difference in memory acquisition as opposed to coping style. Therefore, the Repeated Forced Swim Test (rFST), which reinforces passive coping behavior over multiple trials, was used to determine if *Trip8b*$^{-/-}$ mice show complementary deficits in passive coping while also testing if *Trip8b*$^{-/-}$ mice have improved memory, as reflected in the rate of acquisition of passive coping as compared to wildtype mice. Because the 2w-AA is a simple behavioral task, we also evaluated aggressiveness in the Resident-Intruder Test (RIT) to determine if *Trip8b*$^{-/-}$ mice show increased active coping behavior in a task where behavior is influenced by complex stimuli and other behavioral variables(Koolhaas et al. 2010).

In order to further phenotype the *Trip8b*$^{-/-}$ mice and avoid erroneous conclusions based on Single Point In Time (SPIT) assays, we administered these assays to a naive cohort of *Trip8b*$^{+/+}$ and *Trip8b*$^{-/-}$ mice in sequential order from least to most stressful: RIT, SPBT, and then rFST (Figure 1C). In order to reduce ambiguity between multiple endpoints of coping within each assay, all of the salient endpoints were converted into a z-score based on the normal distribution of the *Trip8b*$^{+/+}$ behavior (detailed description of analysis in methods) to give an “Index” for each assay(Guilloux *et al.* 2011).

Over three daily trials in the RIT, *Trip8b*$^{-/-}$ mice showed shorter attack latencies, increased time spent in offensive aggressive behavior, and an overall higher Aggression Index score (Figure 1D; Supplementary Figure 1). Importantly, neither *Trip8b*$^{+/+}$ nor *Trip8b*$^{-/-}$ mice showed signs of ‘violent aggression,’ as there were no signs of excessive wounding, and rare wounding was mainly on the rump and restricted from sensitive areas (face, neck, genitals, etc). A full description of behaviors during this test are available in the supplementary materials (Supplemental Table 1).

The week following RIT, *Trip8b*$^{+/+}$ and *Trip8b*$^{-/-}$ mice were tested on the SPBT, where *Trip8b*$^{-/-}$ mice displayed less freezing, more burying, and a shorter latency to bury in the Acquisition Trial but no significant changes in the Recall Trial compared to *Trip8b*$^{+/+}$ mice (Supplementary Figure 2, Supplementary Table 2). An “SBPT Index” for each trial was again compiled using z-score normalization (Supplementary Figure 2), while a composite SPBT Index achieved through the average of both trials confirmed that *Trip8b*$^{-/-}$ mice demonstrated more active coping behavior overall in the SPBT (Figure 1E). A “Change in Response” ratio was computed as the difference between the total time spent burying and freezing in the Acquisition and Recall Trial divided by the total time spent burying and freezing in the Acquisition Trial and demonstrated that both groups had similar changes in responses to the environment between trials, suggesting that differences in memory were not responsible for the differences in behavior (Supplementary Figure 2).

Lastly, the rFST was administered to both groups one week following the SPBT. Similar to the classic FST, mice were placed in water for 6 minutes, and their total time spent immobile was recorded. However, this FST procedure was repeated on a second and third day to assess acquisition of passive coping-like behavior as the mouse became familiar with the task. By scoring the last four minutes of the first day's trial, we confirmed prior observations that the *Trip8b*$^{-/-}$ mice spend significantly less time immobile than *Trip8b*$^{+/+}$ counterparts on the "classic" FST (Supplementary Figure 3). In addition, *Trip8b*$^{-/-}$ mice continued to spend less time immobile compared to *Trip8b*$^{+/+}$ controls across all three full rFST trials (Supplementary Figure 3). Both groups spent significantly more time immobile on Trial 3 compared to Trial 1, indicating that while *Trip8b*$^{-/-}$ mice showed a propensity towards more active coping, they were still able to adapt to their environment via acquisition of passive coping in later trials. An average score of the full time spent immobile in each of the three trials was z-score normalized into a "rFST Index", which further confirmed that *Trip8b*$^{-/-}$ mice showed a decreased propensity for passive coping in the rFST (Figure 1F).

The behavior on these three coping assays can be altered by a number of environmental stimuli and can also be influenced by mental processes other than coping style, thus introducing high variability(Guilloux et al. 2011). To better understand *Trip8b*$^{-/-}$ mice's coping style overall, we combined the three indices from the RIT, SPBT, and rFST to create an "Active Coping Index" (ACI) that was equally influenced by all three tests. As predicted, *Trip8b*$^{-/-}$ mice demonstrated higher scores on the ACI than their *Trip8b*$^{+/+}$ counterparts (Figure 1G). Importantly, *Trip8b*$^{-/-}$ mice show similar locomotor and anxiety-like activity behavior compared to *Trip8b*$^{+/+}$ mice (Supplementary Figure 4), and our previous publications have also demonstrated that neither group shows differences in memory(Lewis et al. 2011, Han et al. 2017). Thus, global HCN channel reduction through *Trip8b*$^{-/-}$ leads specifically to increased active coping.

TRIP8b(1b-2) overexpression reduces HCN channels in CA1

Previous studies have shown that the antidepressant-like behavior seen in HCN-KO mice depends on downregulation of I_h specifically in CA1 region (Kim et al. 2017, Han et al. 2017). Therefore, we developed a novel genetic approach (Figure 2A) to target neurons using overexpression of TRIP8b-(1b-2), a dominant negative TRIP8b spliceform(Piskorowski *et al.* 2011, Lewis *et al.* 2009). In addition, we inserted an IRES-GFP after the dominant negative TRIP8b(1b-2) spliceform to track infected cells. We refer to this approach as AAV-(1b-2) and used a negative control vector without the TRIP8b-(1b-2) spliceform, termed AAV-GFP, for comparison.

Using unilateral AAV-GFP and AAV-(1b-2) injections into CA1 of wildtype C57BL/6J mice, we were able to investigate how our genetic approach impacted HCN channel expression and distribution. As expected, we found that HCN1, HCN2, and endogenous TRIP8b was reduced significantly in CA1 of AAV-(1b-2) compared to AAV-GFP injected hemispheres via western blot (Figure 3) and immunohistochemistry (Figure 2B,C). In addition, injection of AAV-(1b-2), but not AAV-GFP, depleted HCN channel expression in distal dendrites of CA1 pyramidal cells, which has previously been shown to influence antidepressant-like behavior(Han et al. 2017).

In addition, we performed somatic whole cell recordings with acutely sliced AAV-GFP and AAV-(1b-2) injected CA1 pyramidal cells. Similar to our protein analysis, we observed a large reduction in the sag ratio (Figure 2D,E) and I_h amplitude (Figure 2F,G) in AAV-(1b-2) injected cells compared to AAV-GFP injected controls. Similar to previous manipulations that reduce I_h in this cell type(Lewis et al. 2011, Kim et al. 2012), we confirmed an increase in the excitability of AAV-(1b-2) injected cells compared to AAV-GFP injected controls (Figure 2H). Overall, these results suggest that AAV-(1b-2) mediated reduction in HCN channels leads to reduced CA1 excitability.

Next, we performed electron microscopy (EM) of serial sections from AAV-GFP and AAV-(1b-2) injected animals to evaluate the subcellular localization of HCN channels in CA1 pyramidal cells (Figure 4). Similar to HCN1 localization in wild-type animals, HCN1 immunoreactivity in AAV-GFP injected CA1 was strongest along the dendritic trunks, especially within the stratum lacunosum moleculare (SLM). Consistent with our biochemical findings, the density of HCN1 particles in the SLM was markedly reduced in AAV-(1b-2) injected hippocampi. Qualitatively, we noticed an increase in HCN1 immunoreactivity within lysosomes in AAV-(1b-2) injected CA1, although the observation of lysosomes were a rare event and precluded exact quantification of the total number of HCN1 channels in lysosomes. However, the absence of endogenous TRIP8b causes lysosome-mediated degradation of HCN channels(Lewis et al. 2011), and *in vitro* work has similarly shown that TRIP8b(1b-2) removes HCN channels from the cell surface(Santoro *et al.* 2004). This subcellular anatomy together with biochemical evidence of decreased protein levels suggests that expression of the TRIP8b(1b-2) spliceform promotes endocytosis of HCN channels from the plasma membrane and redistribution to lysosomes for degradation.

AAV-(1b-2) in the CA1 leads to an increase in active coping

As our AAV-(1b-2) genetic approach reduces I_h in the CA1, we next sought to determine whether this manipulation leads to increased active coping, similar to global *Trip8b*$^{-/-}$. We bilaterally injected AAV-GFP or AAV-(1b-2) into C57BL/6J mice, waited 4 weeks to ensure maximal protein expression in infected neurons, and then assayed these mice on our ACI behavioral battery (Figure 5A). Though AAV-(1b-2) mice exhibited no differences in aggressiveness in the RIT, AAV-(1b-2) mice showed increased active coping and less passive coping in both trials of the SPBT and less passive coping in the rFST (Figure 5B, C, D; Supplemental Figures 6–8 and Supplementary Tables 3 and 4). Combining all three behavioral tests into the ACI demonstrated that AAV-(1b-2) mice showed a more robust active coping response compared to AAV-GFP controls (Figure 5E). As with the *Trip8b*$^{-/-}$ mice, no differences in locomotor, anxiety-like, or memory-related behaviors were noted between AAV-(1b-2) and AAV-GFP injected mice (Supplementary Figure 8). Overall, these results demonstrate that reduction of HCN channels in CA1 pyramidal cells leads to an increase in excitability and active coping (Figure 5F).

Discussion

In the current report, we demonstrate that loss of HCN channel expression in CA1 leads to an increase in active coping behavior. Our work adds to growing literature establishing that

loss of HCN1, HCN2, or TRIP8b in the CA1 of the hippocampus promotes antidepressant-like behavior(Kim et al. 2017, Lewis et al. 2011, Kim et al. 2012, Han et al. 2017). Further, selective loss of HCN1 in the CA1 is able to protect rats from developing these behaviors after chronic mild stress(Kim et al. 2017, Kim et al. 2012). As such, both HCN and TRIP8b are potential targets for new antidepressant treatments, although it may ultimately be the case that manipulating either of these molecular targets has broader effects in promoting active coping behavior(Lyman *et al.* 2017).

Evidence for active coping in Trip8b$^{-/-}$ mice

While the role of HCN channels in CA1 has been described in terms of chronic stress, we wondered how HCN channels may influence coping responses to acute stressors. We demonstrated that *Trip8b*$^{-/-}$ mice, which show a profound reduction in I_h (Lewis et al. 2011), preferentially engage in active coping with presentation of acutely stressful situations, as seen in the first day of the 2w-AA (Figure 1). The 2w-AA is a direct task of active coping, where choosing this style of coping over freezing leads to the adaptive response of avoiding a shock. However, this task is unimodal and favors one style of coping. Therefore, we expanded our description of *Trip8b*$^{-/-}$ mice's coping style to more complex tasks. The SPBT is a neutral task in terms of coping, as either avoidant freezing (passive) or burying (active) are equally adaptive responses to the stressor. The persistent preference for active coping and decreased passive coping in this task demonstrates that *Trip8b*$^{-/-}$ mice do not simply learn to actively cope more quickly but instead choose this strategy given equal options. In contrast, the rFST is a task that favors passive coping, as immobility leads to floating and preservation of energy(de Kloet & Molendijk 2016). *Trip8b*$^{-/-}$ mice display decreased passive coping in this task, again demonstrating that their preference for active coping is not simply a matter of more quickly adapting to a situation, which would have been reflected in more immobility time than wildtype controls on the subsequent days of the rFST. Finally, the RIT assessed coping style in a more species-specific assay. Once again, *Trip8b*$^{-/-}$ mice showed a preference for active coping evidenced by increased aggression without showing signs of pathologically violent aggression. These findings support the assertion that *Trip8b*$^{-/-}$ mice prefer active coping when challenged with an acute stressor.

TRIP8b facilitates HCN channel expression and proper localization in many brain regions, therefore examining *Trip8b*$^{-/-}$ mice precluded us from ruling out developmental sequelae and the effects from loss of TRIP8b in other brain regions. To circumvent these issues, we employed a viral strategy to overexpress a dominant negative TRIP8b isoform, TRIP8b(1b-2), that led to robust downregulation of HCN channels (Figure 2). While the majority of TRIP8b isoforms upregulate HCN channels and increase surface trafficking, TRIP8b(1b-2) is unique in its ability to reduce HCN expression *in vitro*(Lewis et al. 2009) by removing HCN channels from the cell surface(Santoro et al. 2004). Interestingly, corresponding *in vivo* experiments using a GFP-TRIP8b-(1b-2) fusion protein have not produced identical results(Santoro *et al.* 2009). Unlike in heterologous expression systems, viral expression of GFP-TRIP8b-(1b-2) only influenced trafficking of newly synthesized HCN channel subunits, raising the possibility that HCN subunits stably associated with TRIP8b are not amenable to disruption by a dominant negative isoform(Santoro et al. 2009). In the current report, we observed a contrasting result, namely that overexpression of

TRIP8b(1b-2) readily associates with HCN and leads to internalization of the channels. Although there are several possible explanations for the discrepancy between our current results and that of Santoro and colleagues (ie synapsin vs CaMKII promoter, AAV vs lentivirus), it is most likely related to the reduced efficacy of the GFP-tagged construct in the prior report. Importantly, our experiments with AAV-(1b-2) confirmed our hypothesis that loss of HCN channels in CA1 leads to more active coping (Figure 5) and highlighted the importance of this region for regulating coping style.

We observed that expression of AAV-(1b-2) in pyramidal neurons led to a reduction in excitability, and based on prior reports examining the function of HCN channels, we reason that this change in excitability is directly related to the effect of HCN channels on membrane resistance(Piskorowski et al. 2011, Lewis et al. 2009). Our use of a synapsin promoter led to expression of AAV-(1b-2) in interneurons as well, although we argue that this has a minor effect (if any) on our results for the following reasons. In our prior report, we noted that HCN1 channels are expressed in presynaptic inhibitory terminals of CA1 in a TRIP8b-independent manner(Han et al. 2017). In the present report, use of the AAV-(1b-2) construct did not alter the expression of presynaptic HCN1 channels synapsing onto the CA1 cell body layer (see the *stratum pyramidale in* Figure 2). Moreover, we noted identical results in terms of active coping when comparing the *Trip8b*$^{+/+}$ and *Trip8b*$^{-/-}$ mice, where inhibitory neuron HCN channels are intact, and comparing AAV-GFP and AAV-(1b-2), where there may have been an undetected effect on presynaptic HCN1. Therefore, if the AAV-(1b-2) construct had an effect on inhibitory HCN1 channels, it is below the threshold for detection by immunohistochemistry and is unlikely to have influenced the active coping phenotype. Beyond changing the excitability of CA1 pyramidal neurons, it may also be the case that manipulating HCN channels ultimately leads to a change in hippocampal circuit parameters(Yi *et al.* 2016). Although we cannot exclude this possibility, we reason that the discussion above reinforces the importance of postsynaptic changes in HCN channel expression as fundamental to the mechanism linking changes in HCN channel expression to changes in the behavioral phenotype that we observed.

While the most likely mechanism whereby AAV-(1b-2) led to increased active coping involves increased excitability of CA1 pyramidal cells through I_h reduction, there are a few alternatives that should be considered. First, while I_h has independently been shown to influence subcellular excitability in pyramidal cells, it is unclear if such changes in HCN channels influence the expression of other ion channels, which may contribute to the excitability in different subcellular locations along the neuron. In addition, while CA1 excitability was clearly affected by our AAV-(1b-2) approach, it is possible that other cell types within CA1 were affected. Finally, though AAV-(1b-2) increased CA1 excitability, we were unable to predict how other brain regions that are in network with CA1, such as the Lateral Septum, might be affected, raising the possibility that the changes in CA1 excitability indirectly affected coping behavior through broader network changes. Future experiments investigating these alternative mechanisms would be helpful in determining how HCN channels in CA1 pyramidal cells influence coping behavior.

Interpreting HCN Channels' role in psychiatric disease

Previous studies have linked HCN channel activity in CA1 to depression-like behavior, and our current study expands on this by identifying HCN as a regulator of the coping response to acute psychosocial stressors. While active coping has been linked to better outcomes for patients with MDD(Bjørkløf *et al.* 2013, Cairns *et al.* 2014, Southwick et al. 2005), it has also been reported to benefit many other psychiatric diseases, including Bipolar Disorder(Goossens *et al.* 2008), Schizophrenia(Meyer 2001), Substance Abuse and Alcoholism(Humphreys *et al.* 1999, Moser & Annis 1996), and PTSD(Contractor *et al.* 2016). It is notable that active coping has also been shown to benefit patients with non-psychiatric disorders, including chronic illness(Stewart & Yuen 2011), HIV(Gore-felton & Koopman 2008), diabetes(Huang *et al.* 2016), post-stroke recovery(Tielemans *et al.* 2014), and cardiovascular disease(Chiavarino *et al.* 2012). By identifying HCN channel function in CA1 as a determinant of coping strategy, we reason that it could impact the course of disease in many chronic illnesses.

As increasing emphasis has been put on understanding neuropsychiatric disease susceptibility and resilience, researchers have established electrophysiological, genetic, and epigenetic phenotypes that predispose rodents to being susceptible or resilient to developing certain maladaptive behaviors that are similar to human neuropsychiatric diseases (anhedonia, fear-extinction deficits, decreased social interactions, etc.) (Russo et al. 2012). Though multiple molecular mechanisms have been identified as determinants of whether these disease-like behaviors manifest in rodents after stress, few have associated protective or maladaptive behavioral responses with this progression to disease-like phenotypes, and it could be argued that opposing adaptation styles are beneficial in distinct contexts(de Boer *et al.* 2017). Two studies, however, have demonstrated evidence that similar associations between active coping in rodents may be similar to humans: First, rats that displayed more defensive aggressive postures and had longer latencies to submissive postures during social defeat had fewer deficits in social interaction and less pathological neuroendocrine responses to stress(Wood et al. 2010). Second, rat strains that have shown multiple differences in behavior on assays specific to coping style showed marked differences in social interaction behavior as adults when undergoing social defeat as adolescents. In particular, the strain with more active coping showed fewer deficits in social interaction with both a dominant male and female compared to the strain with passive coping (Vidal et al. 2011). Though few in number, these studies begin to demonstrate that rodents also engage in stress-mitigating behaviors that lead to protection against developing maladaptive behaviors, similar to humans. This study adds further support to this evidence, tying promotion of active coping strategies in this study to the resistance to depression-like behavior after chronic stress found in other studies(Kim et al. 2017, Han et al. 2017).

In light of the broad clinical utility of increasing active coping, if mechanisms that influence coping behavior in mice are shared by humans, HCN channels may be a novel therapeutic target to benefit patients with a multitude of diseases in which active coping has been found to be beneficial.

Supplementary Material

Refer to Web version on PubMed Central for supplementary material.

Acknowledgements

This work was supported by National Institutes of Health Grants 2R01NS059934, R01MH106511, R21MH104471 (D.M.C), and F30MH109249 (D.W.F.), Brain Research Foundation SG 2012–01 (D.M.C.), Chicago Biomedical Consortium HTS-004 (Y.H. and D.M.C.), Northwestern University Clinical and Translational Sciences Institute 8UL1TR000150 (Y.H.), and Brain and Behavior Research Foundation NARSAD 25138 (Y.H.). This work was supported by Northwestern University's Center for Advanced Microscopy and a Cancer Center Support Grant (NCI CA060553) as well as Northwestern University's Behavioral Phenotyping Core.

Abbreviations:

(HCN)	Hyperpolarization-activated Cyclic Nucleotide-gated Channel
(I_h)	hyperpolarization-activated current
(TRIP8b)	Tetratricopeptide repeat-containing Rab8b-Interacting Protein
(MDD)	Major Depressive Disorder
(KO)	Knockout
(FST)	Forced Swim Test
(TST)	Tail Suspension Test
(RIT)	Resident Intruder Test
(rFST)	repeated Forced Swim Test
(SPBT)	Shock Probe Burying Test
(2w-AA)	Two-Way Active Avoidance
(ACI)	Active Coping Index
(ZM)	Zero Maze
(MWM)	Morris Water Maze
(OFT)	Open Field Test
(ITI)	Intertrial Interval
(SPIT)	Single-Point In Time assay
(RDoC)	Research Domain Criteria
(TBS)	Tris-Buffered Saline
(STEM)	Scanning Electron Microscope in Scanning Transmission
(EM)	Electron Microscope

(SLM) Stratum Lacunosum Moleculare

References

Arnone D, McIntosh AM, Ebmeier KP, Munafò MR and Anderson IM (2012) Magnetic resonance imaging studies in unipolar depression: Systematic review and meta-regression analyses. European Neuropsychopharmacology, 22, 1–16. [PubMed: 21723712]

Bjørkløf GH, Engedal K, Selbæk G, Kouwenhoven SE and Helvik A-S (2013) Coping and Depression in Old Age: A Literature Review. DEM, 35, 121–154.

Boucher AA, Arnold JC, Hunt GE, Spiro A, Spencer J, Brown C, McGregor IS, Bennett MR and Kassiou M (2011) Resilience and reduced c-Fos expression in P2X7 receptor knockout mice exposed to repeated forced swim test. Neuroscience, 189, 170–177. [PubMed: 21664437]

Brager DH and Johnston D (2007) Plasticity of Intrinsic Excitability during Long-Term Depression Is Mediated through mGluR-Dependent Changes in Ih in Hippocampal CA1 Pyramidal Neurons. J. Neurosci, 27, 13926–13937. [PubMed: 18094230]

Briley M and Lépine (2011) The increasing burden of depression. Neuropsychiatric Disease and Treatment.

Cairns KE, Yap MBH, Pilkington PD and Jorm AF (2014) Risk and protective factors for depression that adolescents can modify: A systematic review and meta-analysis of longitudinal studies. Journal of Affective Disorders, 169, 61–75. [PubMed: 25154536]

Casey BJ, Craddock N, Cuthbert BN, Hyman SE, Lee FS and Ressler KJ (2013) DSM-5 and RDoC: progress in psychiatry research? Nat Rev Neurosci, 14, 810–814. [PubMed: 24135697]

Chiavarino C, Rabellino D, Ardito RB, Cavallero E, Palumbo L, Bergerone S, Gaita F and Bara BG (2012) Emotional coping is a better predictor of cardiac prognosis than depression and anxiety. Journal of Psychosomatic Research, 73, 473–475. [PubMed: 23148818]

Contractor AA, Armour C, Shea MT, Mota N and Pietrzak RH (2016) Latent profiles of DSM-5 PTSD symptoms and the “Big Five” personality traits. Journal of Anxiety Disorders, 37, 10–20. [PubMed: 26561734]

de Boer SF, Buwalda B and Koolhaas JM (2017) Untangling the neurobiology of coping styles in rodents: Towards neural mechanisms underlying individual differences in disease susceptibility. Neuroscience & Biobehavioral Reviews, 74, 401–422. [PubMed: 27402554]

De Boer SF and Koolhaas JM (2003) Defensive burying in rodents: ethology, neurobiology and psychopharmacology. European Journal of Pharmacology, 463, 145–161. [PubMed: 12600707]

de Kloet ER and Molendijk ML (2016) Coping with the Forced Swim Stressor: Towards Understanding an Adaptive Mechanism. Neural Plasticity, 2016, e6503162.

Degroot A and Nomikos GG (2004) Genetic deletion and pharmacological blockade of CB1 receptors modulates anxiety in the shock-probe burying test. European Journal of Neuroscience, 20, 1059–1064. [PubMed: 15305874]

Duman RS and Aghajanian GK (2012) Synaptic Dysfunction in Depression: Potential Therapeutic Targets. Science, 338, 68–72. [PubMed: 23042884]

Duman RS and Monteggia LM (2006) A Neurotrophic Model for Stress-Related Mood Disorders. Biological Psychiatry, 59, 1116–1127. [PubMed: 16631126]

Fan Y, Fricker D, Brager DH, Chen X, Lu H-C, Chitwood RA and Johnston D (2005) Activity-dependent decrease of excitability in rat hippocampal neurons through increases in Ih. Nature Neuroscience, 8, 1542–1551. [PubMed: 16234810]

Goossens PJJ, Klein E. A. M. K. -v. d. and Achterberg T. v. (2008) Coping Styles of Outpatients With a Bipolar Disorder. Archives of Psychiatric Nursing, 22, 245–253. [PubMed: 18809117]

Gore-felton C and Koopman C (2008) Behavioral Mediation of the Relationship Between Psychosocial Factors and Hiv Disease Progression. Psychosomatic Medicine, 70, 569–574. [PubMed: 18519885]

Guilloux J-P, Seney M, Edgar N and Sibille E (2011) Integrated behavioral z-scoring increases the sensitivity and reliability of behavioral phenotyping in mice: Relevance to emotionality and sex. Journal of Neuroscience Methods, 197, 21–31. [PubMed: 21277897]

Han Y, Heuermann RJ, Lyman KA, Fisher D, Ismail QA and Chetkovich DM (2017) HCN-channel dendritic targeting requires bipartite interaction with TRIP8b and regulates antidepressant-like behavioral effects. Molecular Psychiatry, 22, 458–465. [PubMed: 27400855]

Hu H, Vervaeke K and Storm JF (2002) Two forms of electrical resonance at theta frequencies, generated by M-current, h-current and persistent Na+ current in rat hippocampal pyramidal cells. J Physiol, 545, 783–805. [PubMed: 12482886]

Huang C-Y, Lai H-L, Lu Y-C, Chen W-K, Chi S-C, Lu C-Y and Chen C-I (2016) Risk Factors and Coping Style Affect Health Outcomes in Adults With Type 2 Diabetes. Biological Research For Nursing, 18, 82–89. [PubMed: 25670841]

Humphreys K, Mankowski ES, Moos RH and Finney JW (1999) Do enhanced friendship networks and active coping mediate the effect of self-help groups on substance abuse? Ann Behav Med, 21, 54–60. [PubMed: 18425655]

Insel T, Cuthbert B, Garvey M, Heinssen R, Pine DS, Quinn K, Sanislow C and Wang P (2010) Research Domain Criteria (RDoC): Toward a New Classification Framework for Research on Mental Disorders. Am J Psychiatry, 167, 748–751. [PubMed: 20595427]

Kessler Rc BP (2005) LIfetime prevalence and age-of-onset distributions of dsm-iv disorders in the national comorbidity survey replication. Arch Gen Psychiatry, 62, 593–602. [PubMed: 15939837]

Kim CS, Brager DH and Johnston D (2017) Perisomatic changes in h-channels regulate depressive behaviors following chronic unpredictable stress. Molecular Psychiatry.

Kim Chung S., Chang Payne Y. and Johnston D (2012) Enhancement of Dorsal Hippocampal Activity by Knockdown of HCN1 Channels Leads to Anxiolytic- and Antidepressant-like Behaviors. Neuron, 75, 503–516. [PubMed: 22884333]

Koolhaas JM, Coppens CM, Boer S. F. d., Buwalda B, Meerlo P and Timmermans PJA (2013) The Resident-intruder Paradigm: A Standardized Test for Aggression, Violence and Social Stress. JoVE (Journal of Visualized Experiments), e4367–e4367. [PubMed: 23852258]

Koolhaas JM, de Boer SF, Coppens CM and Buwalda B (2010) Neuroendocrinology of coping styles: Towards understanding the biology of individual variation. Frontiers in Neuroendocrinology, 31, 307–321. [PubMed: 20382177]

Krishnan V and Nestler EJ (2008) The molecular neurobiology of depression. Nature, 455, 894–902. [PubMed: 18923511]

Lewis AS, Schwartz E, Savio Chan C et al. (2009) Alternatively Spliced Isoforms of TRIP8b Differentially Control H Channel Trafficking and Function. J. Neurosci, 29, 6250–6265. [PubMed: 19439603]

Lewis AS, Vaidya SP, Blaiss CA et al. (2011) Deletion of the Hyperpolarization-Activated Cyclic Nucleotide-Gated Channel Auxiliary Subunit TRIP8b Impairs Hippocampal Ih Localization and Function and Promotes Antidepressant Behavior in Mice. J. Neurosci, 31, 7424–7440. [PubMed: 21593326]

Lörincz A, Notomi T, Tamás G, Shigemoto R and Nusser Z (2002) Polarized and compartment-dependent distribution of HCN1 in pyramidal cell dendrites. Nature Neuroscience, 5, 1185–1193. [PubMed: 12389030]

Lyman KA, Han Y and Chetkovich DM (2017) Animal models suggest the TRIP8b-HCN interaction is a therapeutic target for major depressive disorder. Expert Opinion on Therapeutic Targets, 21, 235–237. [PubMed: 28127990]

Magee JC (1998) Dendritic Hyperpolarization-Activated Currents Modify the Integrative Properties of Hippocampal CA1 Pyramidal Neurons. J. Neurosci, 18, 7613–7624. [PubMed: 9742133]

Marcelin B, Lugo JN, Brewster AL et al. (2012) Differential Dorso-Ventral Distributions of Kv4.2 and HCN Proteins Confer Distinct Integrative Properties to Hippocampal CA1 Pyramidal Cell Distal Dendrites. J. Biol. Chem, 287, 17656–17661. [PubMed: 22511771]

Mathers CD and Loncar D (2006) Projections of Global Mortality and Burden of Disease from 2002 to 2030. PLoS Med, 3.

Meyer B (2001) Coping with Severe Mental Illness: Relations of the Brief COPE with Symptoms, Functioning, and Well-Being. Journal of Psychopathology and Behavioral Assessment, 23, 265–277.

Moser AE and Annis HM (1996) The role of coping in relapse crisis outcome: a prospective study of treated alcoholics. Addiction, 91, 1101–1114. [PubMed: 8828239]

Narayanan R and Johnston D (2007) Long-Term Potentiation in Rat Hippocampal Neurons Is Accompanied by Spatially Widespread Changes in Intrinsic Oscillatory Dynamics and Excitability. Neuron, 56, 1061–1075. [PubMed: 18093527]

Narayanan R and Johnston D (2008) The h Channel Mediates Location Dependence and Plasticity of Intrinsic Phase Response in Rat Hippocampal Neurons. J. Neurosci, 28, 5846–5860. [PubMed: 18509046]

Nolan MF, Dudman JT, Dodson PD and Santoro B (2007) HCN1 Channels Control Resting and Active Integrative Properties of Stellate Cells from Layer II of the Entorhinal Cortex. J. Neurosci, 27, 12440–12451. [PubMed: 18003822]

Nolan MF, Malleret G, Dudman JT et al. (2004) A Behavioral Role for Dendritic Integration: HCN1 Channels Constrain Spatial Memory and Plasticity at Inputs to Distal Dendrites of CA1 Pyramidal Neurons. Cell, 119, 719–732. [PubMed: 15550252]

Nolan MF, Malleret G, Lee KH et al. (2003) The Hyperpolarization-Activated HCN1 Channel Is Important for Motor Learning and Neuronal Integration by Cerebellar Purkinje Cells. Cell, 115, 551–564. [PubMed: 14651847]

Peña CJ, Kronman HG, Walker DM et al. (2017) Early life stress confers lifelong stress susceptibility in mice via ventral tegmental area OTX2. Science, 356, 1185–1188. [PubMed: 28619944]

Piskorowski R, Santoro B and Siegelbaum Steven A. (2011) TRIP8b Splice Forms Act in Concert to Regulate the Localization and Expression of HCN1 Channels in CA1 Pyramidal Neurons. Neuron, 70, 495–509. [PubMed: 21555075]

Russo SJ, Murrough JW, Han M-H, Charney DS and Nestler EJ (2012) Neurobiology of resilience. Nature Neuroscience, 15, 1475–1484. [PubMed: 23064380]

Santoro B, Piskorowski RA, Pian P, Hu L, Liu H and Siegelbaum SA (2009) TRIP8b Splice Variants Form a Family of Auxiliary Subunits that Regulate Gating and Trafficking of HCN Channels in the Brain. Neuron, 62, 802–813. [PubMed: 19555649]

Santoro B, Wainger BJ and Siegelbaum SA (2004) Regulation of HCN Channel Surface Expression by a Novel C-Terminal Protein-Protein Interaction. J. Neurosci, 24, 10750–10762. [PubMed: 15564593]

Schaefer AT, Angelo K, Spors H and Margrie TW (2006) Neuronal Oscillations Enhance Stimulus Discrimination by Ensuring Action Potential Precision. PLoS Biol, 4.

Southwick SM, Vythilingam M and Charney DS (2005) The Psychobiology of Depression and Resilience to Stress: Implications for Prevention and Treatment. Annual Review of Clinical Psychology, 1, 255–291.

Stewart DE and Yuen T (2011) A Systematic Review of Resilience in the Physically Ill. Psychosomatics, 52, 199–209. [PubMed: 21565591]

Tielemans NS, Visser-Meily JM, Schepers VP, Post MW and Heugten C. M. v. (2014) Proactive Coping Poststroke: Psychometric Properties of the Utrecht Proactive Coping Competence Scale. Archives of Physical Medicine and Rehabilitation, 95, 670–675. [PubMed: 24309070]

Vidal J, Buwalda B and Koolhaas JM (2011) Male Wistar rats are more susceptible to lasting social anxiety than Wild-type Groningen rats following social defeat stress during adolescence. Behavioural Processes, 88, 76–80. [PubMed: 21854839]

Weissman Mm BRC (1996) CRoss-national epidemiology of major depression and bipolar disorder. JAMA, 276, 293–299. [PubMed: 8656541]

Wood SK, Walker HE, Valentino RJ and Bhatnagar S (2010) Individual Differences in Reactivity to Social Stress Predict Susceptibility and Resilience to a Depressive Phenotype: Role of Corticotropin-Releasing Factor. Endocrinology, 151, 1795. [PubMed: 20160137]

Yi F, Danko T, Botelho SC, Patzke C, Pak C, Wernig M and Südhof TC (2016) Autism-associated SHANK3 haploinsufficiency causes Ih channelopathy in human neurons. Science, 352, aaf2669. [PubMed: 26966193]

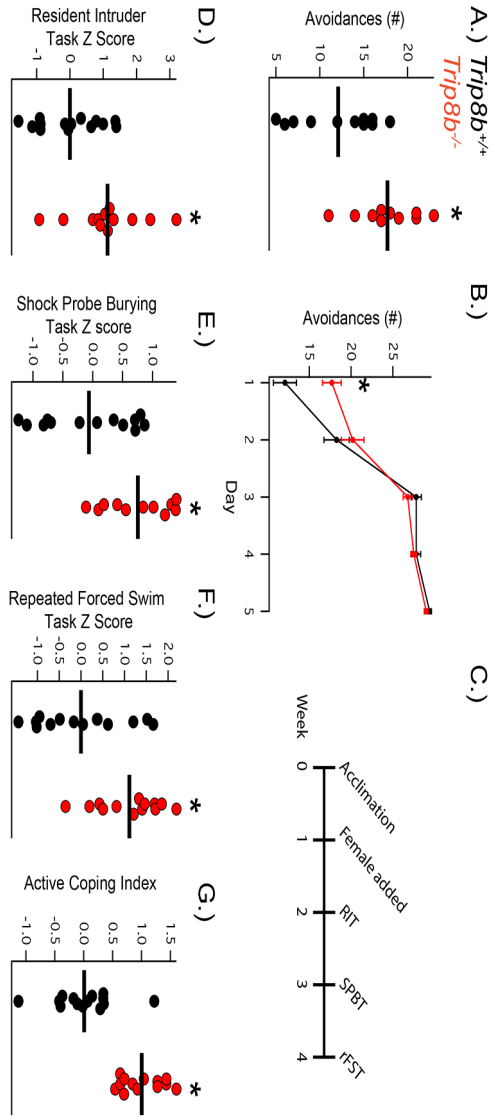

Figure 1: *Trip8b*$^{-/-}$ mice display enhanced active coping.

A) *Trip8b*$^{-/-}$ mice show increased active coping through increased avoidances (t_{19} = 3.113, $p < 0.01$, $n_{subjects}$ = 11,10) on the first day of the Two-Way Active Avoidance Test (2w-AA) with **B)** similar learning of the 2w-AA compared to *Trip8b*$^{+/+}$. **C)** Timeline of Active Coping Index (ACI) behavioral testing. **D)** *Trip8b*$^{-/-}$ mice display more active coping on the Shock Probe Burying Test (t_{22} = 2.914, $p < 0.01$, $n_{subjects}$ = 13, 11), **E)** repeated Forced Swim Test (t_{25} = 3.256, $p < 0.01$, $n_{subjects}$ = 14, 13), and **F)** Resident Intruder Test (t_{24} = 2.819, $p < 0.01$, $n_{subjects}$ = 14, 12). **G)** *Trip8b*$^{-/-}$ mice display greater overall active coping on the ACI (t_{25} = 5.604, $p < 0.0001$, $n_{subjects}$ = 14, 13).

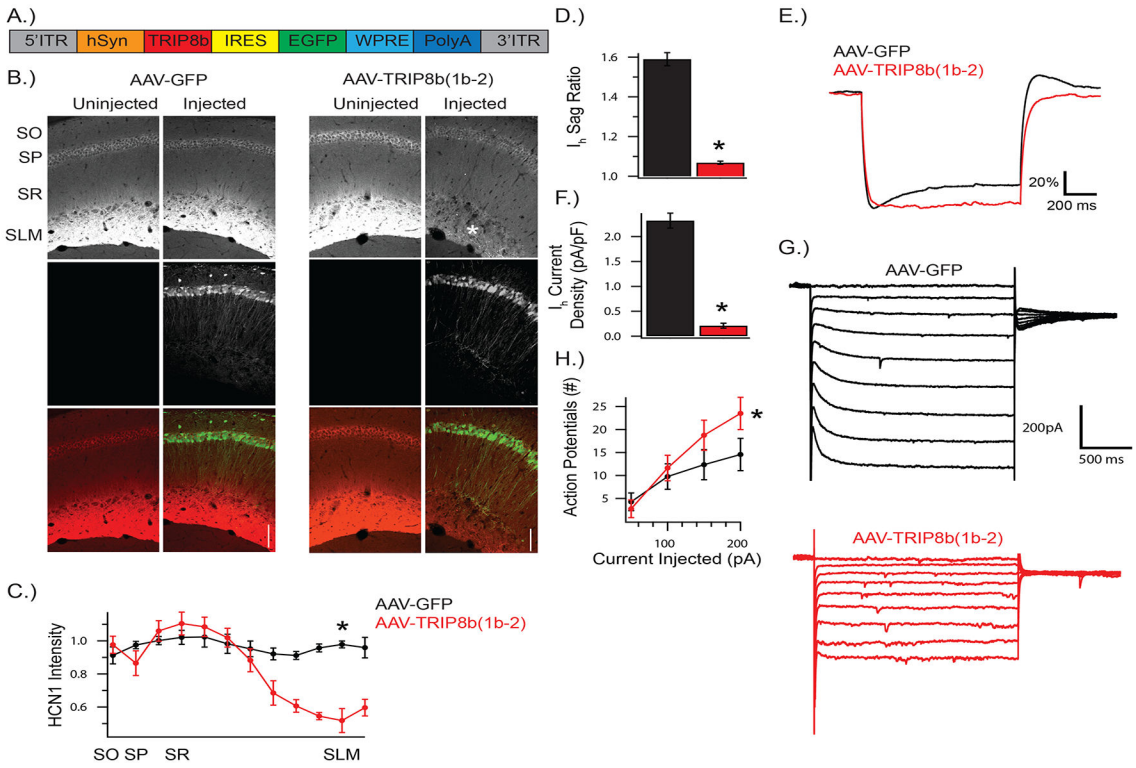

Figure 2: AAV-(1b-2) reduces HCN channels in the CA1.

A) Schematic of AAV-(1b-2). TRIP8b(1b-2) is driven by a human synapsin (hSyn) promoter with IRES-GFP to track infected cells. AAV-GFP expresses GFP through hSyn and lacks TRIP8b(1b-2). **B, C)** HCN1 is reduced in CA1 cells, especially at the distal dendrites (t_4 = 7.712, $p < 0.01$; $n_{subjects}$ = 3,3). Asterisk highlights SLM, where HCN1 is reduced after AAV-(1b-2) injection. **D,E)** Membrane response to a 1s long −200pA current injection from a resting potential of −70mV. Voltage shown is scaled to ΔV_{max} to facilitate comparison of sag ratio amongst conditions. AAV-(1b-2) injected cells show reduced sag ratios compared to AAV-GFP (t_{14} = 14.9, $p < 0.001$, n_{cells} = 8, 8). and **F,G)** I_h current density (t_{13} = −12.0, $p < 0.001$, n_{cells} = 8, 7), and **H)** increased excitability (Repeated Measures ANOVA; genotype × stimulus interaction $F_{3,42}$ = 8.44, $p < 0.001$, n_{cells} = 8, 7). SO: *stratum oriens*, SP: *stratum pyramidale*, SR: *stratum radiatum*, SLM: *stratum lacunosum moleculare*.

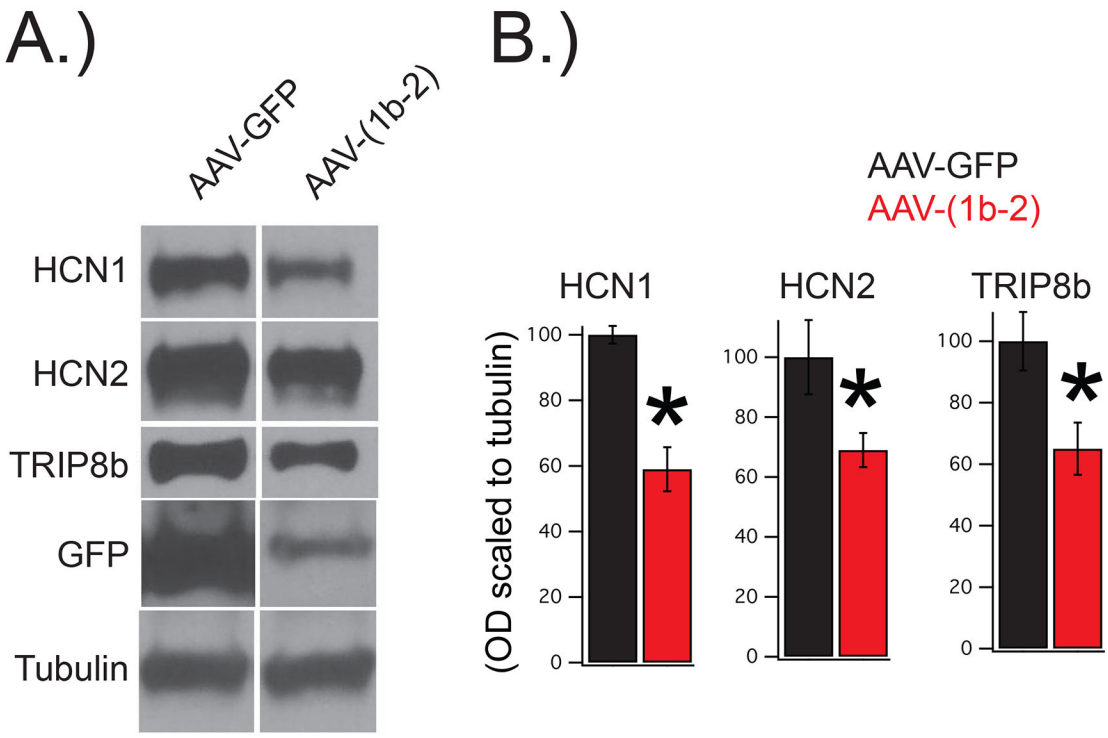

Figure 3: AAV-(1b-2) injection leads to a reduction in HCN1, HCN2, and TRIP8b protein.

Wild type mice were bilaterally injected with either AAV-(1b-2) or AAV-GFP. Four weeks later their hippocampi were sub-dissected for western blot. **A.)** Representative images. **B.)** Quantification of the results reveal reduction in HCN1 (AAV-GFP:100±2.7%, AAV-(1b-2: 59±6.7%,$n_{subjects}$ = 9,12, t_{19}=4.93, p<0.01), HCN2 (AAV-GFP:100±12.3%, AAV-(1b-2: 69±5.7%,$n_{subjects}$ = 8,11, t_{17}=2.45, p<0.05), and total TRIP8b (AAV-GFP:100±9.5%, AAV-(1b-2: 65±8.5%,$n_{subjects}$ = 10,12, t_{20}=2.76, p<0.05) in the AAV-(1b-2) injected mice compared to the AAV-GFP controls.

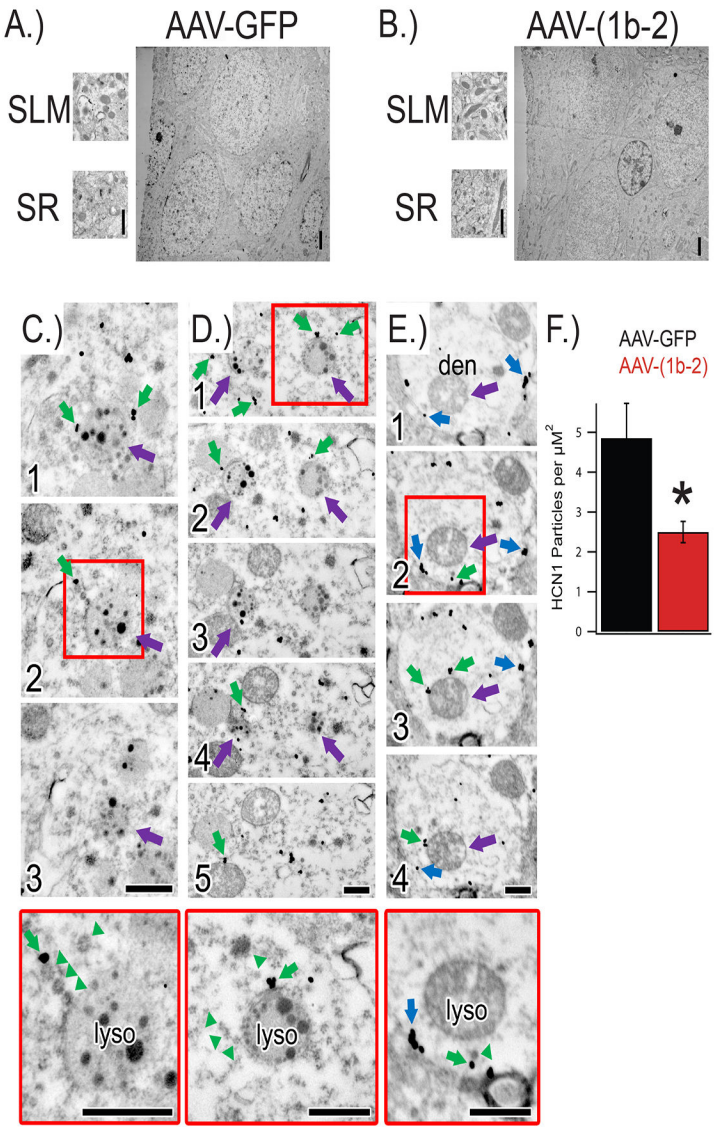

Figure 4: AAV-(1b-2) re-localizes HCN channels to lysosomes for degradation.

A,B) Electron micrographs of hippocampi injected with either AAV-GFP or AAV-(1b-2). **C)** Electron micrographs of serial sections (1, 2, 3) through a lysosome near the soma (purple arrow) in close proximity to endosomes immunoreactive for HCN1 (immunogold particles; green arrows) in the AAV-(1b-2) injected hippocampi. Red box denotes approximate region shown at higher magnification in bottom panel. Note the ordered manner in which the endosomes are lined up near the lysosome (green arrowheads). **D)** Electron micrographs of serial sections (1, 2, 3, 4, 5) through two lysosomes near the soma (purple arrows) with endosomes immunoreactive for HCN1 (green arrows) nearby. **E)** Electron micrographs of serial sections (1, 2, 3, 4) through a spiny dendrite in the stratum lacunosum-moleculare. Despite a dramatic HCN1 decrease in the distal dendrites and the majority of HCN1 immunoreactivity localized to endosomes (green arrows) near lysosomes (purple arrows), occasional cell membrane-bound HCN1 was noted (blue arrows). Higher magnification

images reveal orderly queuing near the lysosome (green arrowheads). Scale bars = 500nm. **F.)** Quantification of HCN1 particle density in the SLM. AAV-GFP 4.85±0.87 particles/μm^2 dendrite, AAV-(1b-2) 2.49±0.26, *$p<0.05$ two tailed T test, $n_{subjects} = 2$, $n_{dendrites} = 22,23$.

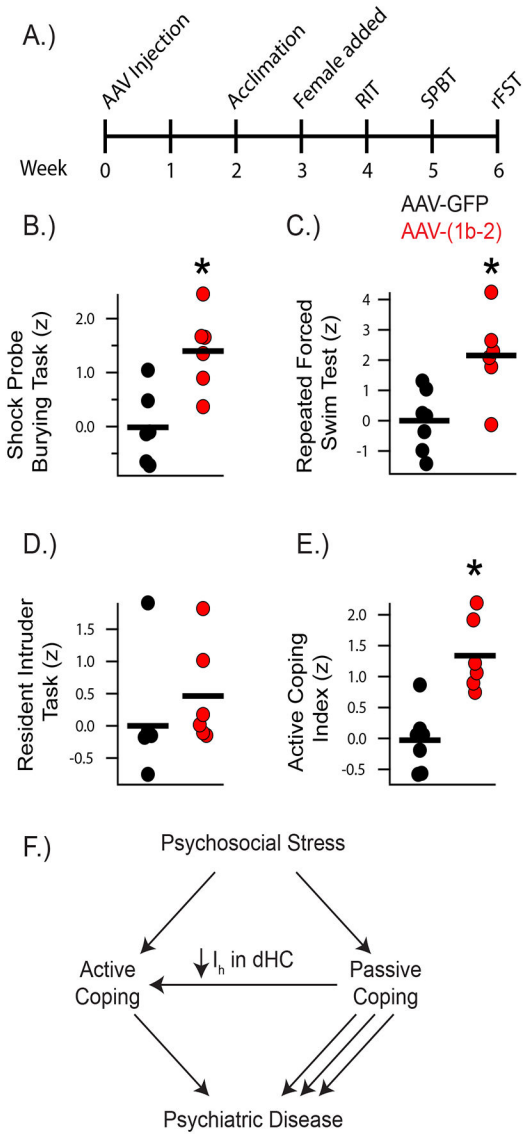

Figure 5: AAV-(1b-2) injection in the CA1 leads to active coping.

A) Timeline of viral injections and Active Coping Index (ACI) behavioral assays. **B)** AAV-(1b-2) mice showed increased active coping in the Shock Probe Burying Test (AAV-GFP: −0.01±0.27, AAV-(1b-2): 1.39±0.29, $t_{10} = 3.510$, $p < 0.01$, $n_{subjects} = 6, 6$). **C)** AAV-(1b-2) mice showed decreased average immobility time across the three repeated Forced Swim Test trials (AAV-GFP: 172.38±10.48s, AAV-(1b-2): 112.61±16.00s $t_{11} = 3.212$, $p < 0.01$, $n_{subjects} = 7, 6$). **D)** AAV-(1b-2) mice did not demonstrate statistically different z-scores from AAV-GFP mice in the Resident Intruder Test (AAV-GFP: 0±0.40, AAV-(1b-2): 0.46±0.32, $t_{10} = 0.8968$, $p > 0.05$). **E)** AAV-(1b-2) mice show enhanced active coping compared to AAV-GFP mice on the ACI ($t_{11} = 4.586$, $p < 0.001$, $n_{subjects} = 7, 6$). **F)** Working model of how HCN Channel loss in the hippocampus leads to increased active coping. When an individual encounters acute psychosocial stress, they cope passively or actively. Those with Active Coping styles tend to be more resistant to developing most neuropsychiatric disorders and

tend to do better with treatment than those who employ Passive Coping styles. Reduction of HCN channels and HCN channel current (I_h) specifically in the CA1 facilitates Active Coping strategies.